Real-World Interference Impacts Analysis using High Dynamic Range GNSS RF/IF Signals Record and Playback

Iurie Ilie, Dominique Fortin

Averna

René Jr. Landry, Marc-Antoine Fortin

École de technologie supérieure

Technical paper

measure. improve. succeed.

Table of Contents

List of Tables and Figures

ABSTRACT

Robustness consideration in GNSS receivers' design and validation still represent a big challenge as multiple RF sources must coexist in an overloaded RF world. Despite the advantages of spectrum spreading techniques used in GNSS, receivers are still vulnerable to interferences generated by a variety of sources (FM/TV transmitters' harmonics, mobile phone networks, AM transmitters, location based services transmitters, etc.). Most of the research and analysis done in this area are based on the GNSS simulators. Simulated GNSS signals are combined with RF interferences at the GNSS receiver RF input, bypassing the active GNSS antenna. Although very efficient, these methods still lack reproducing real-world signal impairments with high fidelity. To complete the analysis of GNSS receivers' performance in presence of interferences and to have a better understanding of the interferences' impacts on real-world GNSS signals, field tests are mandatory. The interferences' impact on GNSS signals analysis in the field is not always easy to perform in real-time, especially when the experiment conditions are subject to constant changes. Also, field tests are usually cost- and time-consuming (e.g. flight tests, special environments, complex scenarios, repeatable tests and controlled conditions, etc.). In the proposed interferences' analysis approach, the real GNSS and interference signals are first recorded with a Multi-frequency Record and Playback system (like a snapshot of the real-world RF spectrum) in a large frequency band with a high dynamic range. The recorded data (GNSS plus interference signals) are post-processed in order to analyze the GNSS signal degradation and to characterize the nature of the interferences dropped into the GNSS spectrum (out of band interferences are considered). The real-world RF signals, once recorded can be replayed at any time in a controlled environment for any GNSS receiver testing, proof of concept and demonstrations or technological breakthrough

1. INTRODUCTION

This paper introduces the Multi-frequency RF Signal Record & Playback System (MF R&P) applied to interferences impact analysis on the GNSS field. The first section briefly describes the MF R&P and presents the typical setup examples for GNSS applications. This setup is focused on applications requiring multiple frequencies/channels recording and playback. The next sections present the methodology used for interferences analysis and the validation of the approach is described. A final section describes the tests done with UHF CH 23.

2. MULTI-FREQUENCIES RECORD & PLAYBACK OVERVIEW

The MF R&P is built on the National Instrument (NI) 18-slot PXI-1075 Express chassis with external (or internal) storage devices and pre-amplifiers. MF R&P contains multiples recording (PXI-5663) or/and playback (PXI-5673) modules that are synchronised with a reference 10 MHz clock. T-clock capabilities insure the synchronous and coherent recording and playback of the processed signals. Detailed description of the T-clock can be found in [1]. The PXI equipment is the heart of the system with a chassis, a controller and the recorder and playback modules.

The NI PXI-5663 recording module [2] contains a local oscillator (PXI-5652), a wideband RF downconverter (PXI-5601) and a 16-bit IF digitizer (PXI-5622). Signals with 50 MHz of bandwidth can be recorded at any carrier frequencies of the GNSS spectrum. The NI PXI-5673 playback module [3] contains a local oscillator (PXI-5652), a 16-bit arbitrary waveform generator (PXI-5450) and an I/Q modulator (PXI-5611). Signals of up to 100 MHz of bandwidth can be generated in the 85 MHz to 6.6 GHz frequency range. This allows the playback of the recorded signal on a frequency different from the recorded one (e.g. recorded GPS L1 signals to be replayed on L2 or the IF specific to each GPS receiver frequency).

With external high-throughput storage devices (e.g. FirmTek SeriTek/2EN2 or OSS-PCIe-3U-RAID-12-x4), the PXI-1075 can handle up to 5 recording modules (PXI-5663) or up to 4 playback modules (PXI-5673). Different combinations of recording and playback modules are also possible.

The block diagram (Figure 1) shows the main components of the MF R&P for two channels tuned on the same frequency (GPS L1). RF signals from multiple antennas, once converted to baseband, are stored as 16-bit IQ samples. When two different frequencies are processed (e.g. GPS L1/L2) there are two additional LO (PXI-5652) in the setup (Figure 2). With a complex 25 MS/s (IQ samples) sampling rate, 20 MHz of bandwidth is recorded by each recording module. With such a throughput, nearly 4 hours can be stored on a 2TB device. Multiple storage devices (e.g. SATA 3.5" disk of 1 TB) can be used to record longer periods of time, if required by the application.

A pre-amplifier with manual or Automatic Gain Control (AGC) ensures that the gain is optimized for a maximum dynamic range and linearity. This is notably important when the GPS signal is recorded in presence of interferences [4].
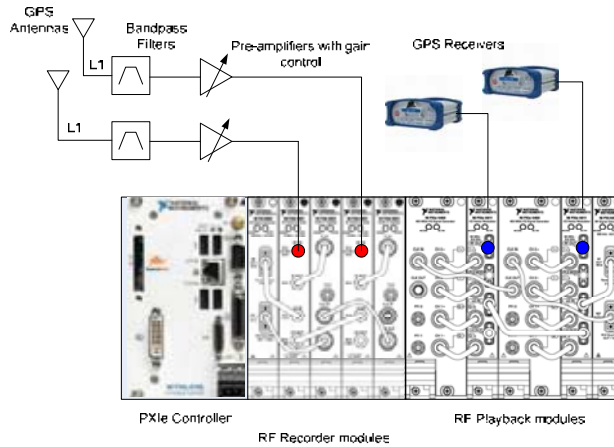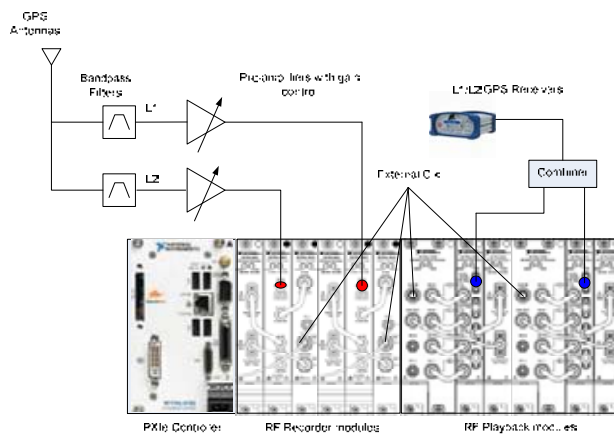
Figure 1 Multi-channels R&P system

Figure 2 Multi-frequency R&P system

This Averna's unit comes with a built-in Low Noise Amplifier (LNA) and can be configured in various ways to accommodate passive or active antennas as well as external components [5]. A band pass filter is mandatory to avoid out of band high power interferences such as cellular network emissions.

The RF R&P has a special algorithm to play back the signal at the same level it was recorded at the RF input. The pre-amplifier can be configured with or without the LNA. While some types of RF signals require Automatic Gain Control, recording GPS signals represents a simpler challenge since the input power level is mostly constant, regardless of the location. The RF Record & Playback can reliably record other types of signals in navigation testing such as GPS assistance data through cellular phone network. Pre-recorded files can be read from the 2 TB storage devices via the Serial ATA interface.

Table 1 Main MF R&P hardware specifications

Parameters	Values
Frequency range	Recorders: from 10 MHz to 6.6 GHz Players: from 85 MHz to 6.6 GHz
Signal bandwidth	Recorders: up to 50 MHz Players: up to 100 MHz
ADC and DAC	16 - bits
Number of modules in PXI-1075 chassis	Up to 5 recording modules OR Up to 4 player modules
T-clock synchronization (between any two modules)	< 0.1ns
Frequency fine tuning resolution	< 300nHz for recording < 400nHz for playback Note: The 400nHz frequency error translates into 0.3mm/hour of GPS L1 carrier phase accumulation)
Phase Noise (10 kHz)	< -105dBc/Hz
Dynamic range	> 80 dB
External reference clock	10 MHz

Table 1 summarizes the main specifications of the hardware used (PXI-1075 + PXI-5663 + PXI-5673). The selected parameters will directly influence the GNSS signal processing during the record and playback routine. For example, large bandwidths allow preservation of the processed signal's shape, high frequency resolutions insure the good phase coherence properties and channels synchronisation keep the time offset between signals in the ranges specified by the GNSS Interface Control Documents.

2.1 Configuration for GNSS Signals

GNSS signals have very weak power, compared to the RF signals used for audio or video broadcasting. For example, the nominal power for GPS L1-C/A signal is -130dBm at a ground-based antenna's input. For this reason, when recording GPS signals, the R&P system is used with the LNA and pre-amplifier. The pre-amplifier can be set for maximum gain in manual mode, or the AGC can be turned on. Active GNSS antennas should be connected to the RF input of the pre-amplifier. The GNSS antenna can be powered from the DC bias included in the pre-amp for powering external active antenna.

Two different approaches can be used for GNSS multi-channels recording. Multiple RF signal recording is possible 1) with same carrier frequency (e.g. GPS L1 + GPS L1 + …+ GPS L1 for a multi-GPS L1 antennas acquisition) or 2) with different carrier frequencies (e.g. GPS L1 + GPS L2P + …+ GPS L5). For the first approach, the same LO can be shared for better phase coherence and less phase noises. In fact, PXIe-5601 as well as PXIe-5611 has LO OUT connectors. This connector enables phase coherent operation of multiple devices by allowing the use of a common LO signal when "daisy-chaining" the signal to other NI 5601 RF Down-converters or NI 5611 I/Q Vector Modulators. The second approach (Figure 3 and 4) supposes multiple LO usage (different LO for each RF signal recorded). In this case, the phase coherence and digitizers' synchronisation is achieved through T-clock synchronisation process.

When synchronously recording two or more GNSS frequencies (e.g. GPS L1 and L2), it is very important not to degrade the time delay and phase coherence. In fact, 1ns of non countable time delay (between two or more recording channels) is equivalent to an error of ~0.3m in pseudorange measurements. For this reason, all connectors used for time synchronisation and RF inputs should be calibrated.

MF R&P can be used in two different configurations based on a) 10 MHz clock synchronization setup and b) local oscillators' setup.
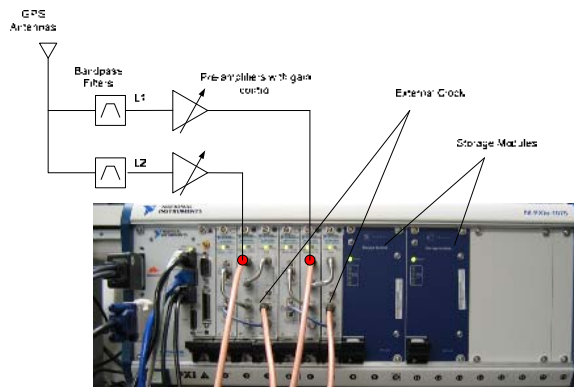

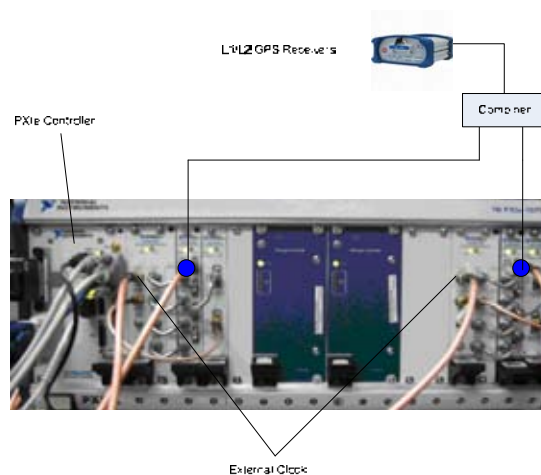*Figure 3 Record configuration for GPS L1/L2*

Figure 4 Playback configuration for GPS L1/L2

The MF R&P is synchronized in three possible ways: by external clock connected to the front panel modules, by an external clock connected to the backplane REF IN connector and by an internal clock source. For better results, the synchronization using the front panel is recommended. As was mentioned previously, the local oscillator can be shared by multiple modules tuned to the same frequency (recording or playback modules) or in multi-frequency mode where each local oscillator is tuned for different frequencies.

3. TEST METHODOLOGY

Potential sources of unintentional interferences to GPS L1 (in the area) are first identified. The information about the transmitter is collected (e.g. frequency spectrum and time domain signal structure). The selected interference is simulated in the lab and the interferences' impacts on the GPS L1 spectrum are analyzed. This is done in order to tune the setup (configuration of MF R&P, preamplifier's gain, logistic, etc.) and to validate the approach. The collected data is post-processed in Matlab. For analysis, the correlation between the recorded out of band interference and the recorded composite (GPS L1 + interference in GPS L1 band) signal is used. The interference is identified in the GPS L1 band using the correlation properties of periodic signals. The analyzed interference is recorded at a 525.14 MHz central frequency (in order to align the spectrums: 525.14 x 3 = 1575.42) and the GPS L1 signal, at 1575.42 MHz.

4. CORRELATIOIN PROPERTIES OF PERIODIC SIGNALS

Generally speaking, cross-correlation is a quantity that measures the similarities between two signals. The value of cross-correlation depends not only on the similarity of the signals, but also on their magnitudes. The cross-correlation function has some properties that are directly applied to our analysis [6]. Mainly:

- The value of the autocorrelation function at the origin is equivalent to the signal normalized power (for periodic signals);
- Maximum value of cross-correlation function is equivalent to the normalized cross-power between two signals;
- If two signals are periodic with the period T, the cross-correlation function is also periodic with the same period T.
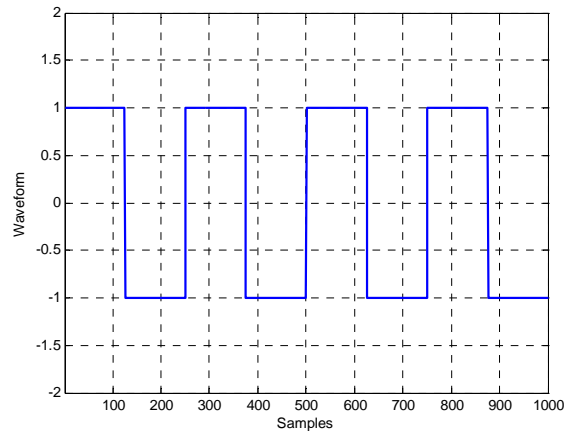
Correlation function is widely used in signal analysis and it is the basic principle used in a GPS receiver. It is extremely useful for the detection and recognition of signals masked by all kinds of additive noise. Lets suppose for instance that we have two digital waveforms: $x(n)$ and $y(n)$. The cross-correlation function $r_{xy}(l)$, based on [7] is defined by:

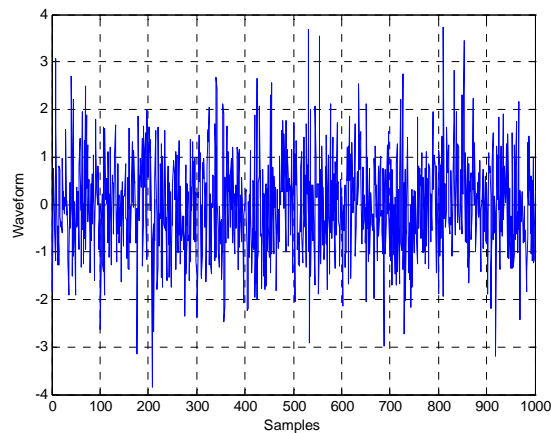$$r_{xy}(l) = \sum_{n=-\infty}^{n=\infty} x(n) * y(n-l) \qquad (0.1)$$

As an example of application of cross-correlation, let us choose a rectangular pulse for $x(n)$ and let us specify the second signal as

$$y(n) = k \cdot x(n) + v(n) \qquad (0.2)$$

where k is a multiplication coefficient, such that $0 < k < 1$. Let us name the product $k{\cdot}x(n)$ the replica signal. The last term, $v(n)$ represents the white noise. The waveforms of the signals as well as the autocorrelation and cross-correlation functions for respective signals are presented in Figures 5 and 6. As it can be noticed, cross-correlation product clearly shows the same pattern as the autocorrelation function for the waveform presented (Figure 6a and Figure 6c).
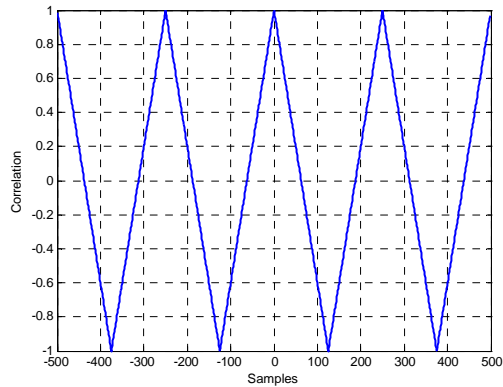

(a)

(b)

Figure 5 Waveforms: a) x(t) - rectangular pulses and b) y(t) – rectangular pulses + noises
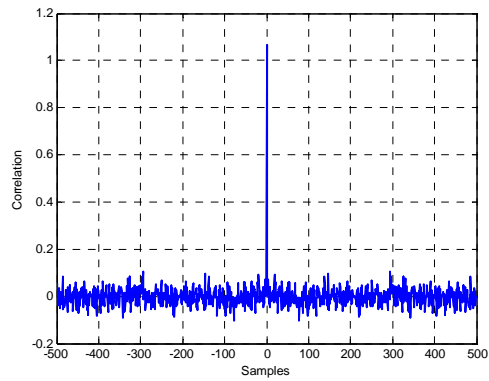
Let us compute the power of the replica (attenuated fundamental signal) using cross-correlation and autocorrelation properties. Let suppose that our $x(n)$ and $y(n)$ are synchronous and $y(n)$ is defined as in equation 1.2. In this case, the cross-correlation peak at the origin ($l = 0$) which is the cross-power [8], is defined as

$$r_{xy}(0) = \sum_{n=-\infty}^{n=\infty} x(n)\,y(n) \qquad (0.3)$$

Substituting (1.2) into (1.3), we obtain equation (1.4). Multiplier k can be found from the ratio between the cross-correlation and autocorrelation peaks (equations 1.5-1.6). As multiplier k represents the amplitude attenuation between the fundamental (x) signal and its replica $(k{\cdot}x)$ signal, the power ratio between these two signals (P_{kx} for replica and P_x for fundamental) can also be found [7] (expression 1.7).

(a)

(b)

(c)

Figure 6 Correlation functions: a) autocorrelation of x(t), b) autocorrelation of y(t) and c) cross-correlation between x(t) and y(t)

$$r_{xy}(0) = \sum_{n=-\infty}^{n=\infty} x(n)[k \cdot x(n) + v(n)] =$$

$$= k \cdot \sum_{n=-\infty}^{n=\infty} x(n)x(n) + \sum_{n=-\infty}^{n=\infty} x(n)v(n) \qquad (0.4)$$

$$= k \cdot r_{xx}(0) + r_{xv}(0)$$

$$\frac{r_{xy}(0)}{r_{xx}(0)} = \frac{k \cdot r_{xx}(0) + r_{xv}(0)}{r_{xx}(0)} = k + \frac{r_{xv}(0)}{r_{xx}(0)} \qquad (0.5)$$

$$k = \frac{r_{xy}(0)}{r_{xx}(0)} - \frac{r_{xv}(0)}{r_{xx}(0)} \qquad (0.6)$$

$$\frac{P_{kx}}{P_x} = \frac{\lim_{N \to \infty} \frac{1}{2N+1} \sum_{n=-N}^{N} |k \cdot x(n)|^2}{\lim_{N \to \infty} \frac{1}{2N+1} \sum_{n=-N}^{N} |x(n)|^2} = k^2 \qquad (0.7)$$

One has to be very careful with the estimation of the multiplier coefficient k. As it is shown in (1.6), there is a $r_{xv}(0)/r_{xx}(0)$ residual that can add non negligible error if not accounted for. In the measurements, the cross-correlation value r_{xy} has to be averaged to minimize the impact of the noise ($r_{xv}(0)$ has a random behavior).

Let us summarize the example shown above. If the autocorrelation function of the fundamental (initial) signal and the cross-correlation function between fundamental and composite (attenuated fundamental + additive noises) are known, one can estimate the power of the fundamental replica in the composite signal. Also, the shape of the fundamental signal can be identified. This principle can also be applied to the out-of-band interference impact analysis to GNSS receivers.

For example, consider as fundamental signal the powerful UHF TV transmitter. As seen by the receiver input, composite signal in this case represents a sum of amplified GNSS signal, harmonics from fundamental UHF TV and additive noise. Once recorded, fundamental signal is cross-correlated with composite received signal and the type of interference as well as the interference power inside the composite signal can be identified. The direct cross-correlation between the out-of-band interference and composite GNSS signal is possible based on the particular properties of the video signal in use. This is explained more closely in the following sections.

5. GNSS SOURCES OF INTERFERENCES

There are multiple sources of unintentional interferences for GNSS. For example for GPS L1, any powerful transmitters that emit n-order harmonics in the 1575.42 MHz ± 10 MHz band have to be considered. For the purpose of this paper, the interference analysis is limited to GPS L1 band. The

source of potential interferers are well described in the literature (e.g. [9], [10]) and papers (e.g. [11]). These can include UHF/VHF TV stations, maritime/military communications, VHFCOM, FM, etc.

Let us focus the present analysis on UHF TV transmitters. Table 2 summarizes the potential interferers generated by broadcasting TV stations (analysis is limited to second and third harmonic only). Let us see more in details the selected UHF TV channels. These channels can be analog or digital (depending of the countries transition plan to digital standard). In Canada, the transition is scheduled to be completed by august, 2011. So, there are still analog TV transmitters in the area. Analog transmitters are more powerful than digital ones and are more likely to interfere with the GPS band. In the analog television network, in North America, the NTSC is used as color TV signal standard. The energy in the NTSC signal spectrum is not distributed uniformly.

Table 2 Potential UHF TV Interferences Sources

Frequency component in the middle of GPS L1 spectrum (MHz)	Potential Sources and Frequencies [MHz]	Comments
L1/3 = 525.14	**UHF CH 22 (518-524)** Video carrier: 519.25 Burst subcarrier: 522.83 Audio carrier: 523.75 **UHF CH 23 (524-530)** Video carrier: 525.25 Burst subcarrier: 528.83 Audio carrier: 529.75	Third harmonic
L1/2 = 787.71	**UHF CH 66 (782-788)** Video carrier: 783.25 Burst subcarrier: 786.83 Audio carrier: 787.75 **UHF CH 67 (788-794)** Video carrier: 789.25 Burst subcarrier: 792.83 Audio carrier: 793.75	Second harmonic

Most of the energy is concentrated on the video carrier, color burst subcarrier and audio carrier. Video carrier is the most powerful one. From Table 2 it can be observed that the video carrier of UHF TV channel 23 is very close to the GPS L1 frequency, if its third harmonic is considered. More precisely, the third harmonic is 525.25 x 3 = 1575.75 (MHz). This corresponds to the 33 spectral line of the C/A code (1575.75MHz – 1575.42MHz = 0.33MHz). The next sections consider the UHF TV channel 23 as the main source of interferences.

5.1   INTERFERE SIGNAL' STRUCTURE

Time domain representation of the NTSC signal is shown on Figure 7. At any time, there are three periodic signal components that are present in the signal (not dependent of the picture to be transmitted): vertical scanlines at 59.94 Hz, horizontal scanlines at 15.7 kHz and the color subcarrier at 3.579545 MHz.

This information is used for interference identification in the GPS L1 composite signal (GPS L1 + interference + noise). In fact, the autocorrelation function for periodic signals is a series of peaks spaced by the period of the signal. Thus, it is expected that the autocorrelation function of the interference used, contains series of peaks spaced by ~1/60s, ~$1/15.7x10^3$s and ~$1/3.58x10^6$s.   .

The spectrum of the expected interference signal is presented in Figure 8. It can be seen that the main energy in the signal spectrum is concentrated on the video carrier and color burst subcarrier (audio component is not took into account). Only periodic signals are considered here.
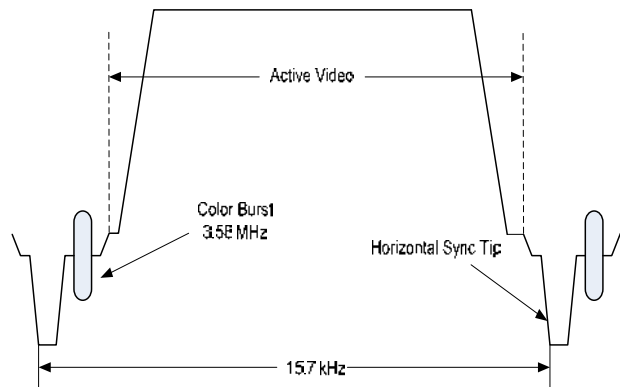

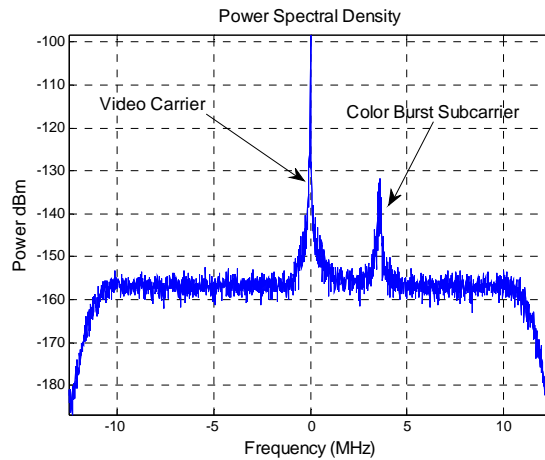*Figure 7 NTSC signal in time domain*

Figure 8 NTSC signal spectrum

5.2   VALIDATION OF HARMONIC GENERATION

Let us suppose that from the transmitter side (source of interferences) all harmonics are properly filtered to the negligible level. Only the fundamental frequencies are present at the GPS antenna input. For the test purpose, two active GPS antenna are used: (A) the high-end GPS antenna for high precision survey applications and (B) mass-market GPS L1 antenna. For simplicity, let us denote the antennas (in order) as A and B. The main components for an active GPS antenna are LNA and RF band-pass filters. It is expected that due to the limited antenna size, the RF built-in filters have a poor attenuation capabilities for out-off band signals.

The typical out off band attenuation for antenna B is -30dB ($f_0 \pm$ 100MHz) and for antenna A is -70 dB ($f_0 \pm$ 100MHz). With very strong power of UHF TV (e.g. channel 23), the interferer's signal can still infiltrate at the active antenna LNA input and, due to nonlinearity of the amplifier circuitry, generate harmonics of the fundamental frequencies. Let us verify this assumption in a controlled environment first. Figure 9 shows the setup used for this first experiment. Based on the knowledge of the interference used (analog UHF TV channel 23), the most powerful components are video carrier at 525.25 MHz, and color burst subcarrier at 528.83 MHz. As it is shown on Figure 8, the color burst subcarrier is at least 20dB lower than video carrier. We use this particularity in the proposed first test.

The Waveform Generator 1 generates a CW1 at 525.25 MHz with 15 dBm of power. The second generator (Waveform Generator 2) produces a CW2 with 3.58 MHz away from the CW1 (528.83 MHz) and with power level adjusted to -5 dBm.
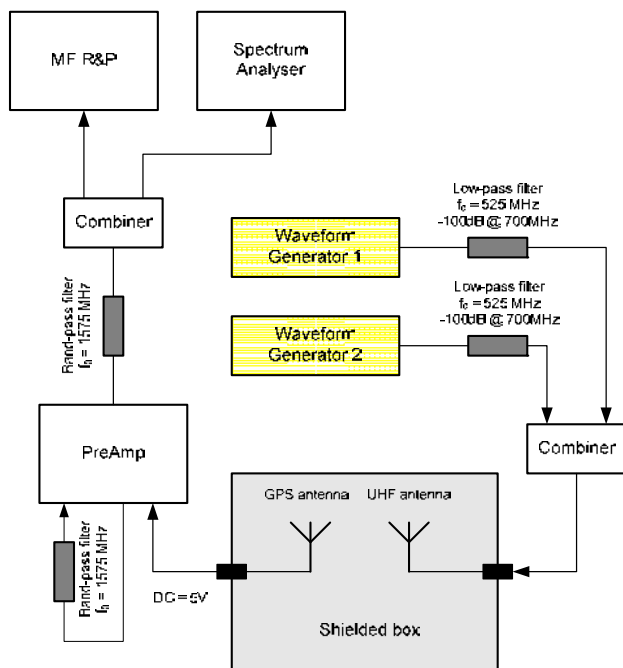
Figure 9 Test setup 1

In order to avoid the harmonic in the transmitted signal, the two band-pass filters are used (more than 100 dB of attenuation). The two CW signal sources are combined and connected with the UHF antenna.

To avoid the uncontrolled emissions, the GPS and the UHF antenna are placed into the shielded box. The active GPS antenna is connected to the DC port of the preamplifier. To avoid infiltration of the generated UHF signal (on the fundamental frequency) into the preamplifier, a band-pass filter (f_0 = 1575 MHz) is used. The preamplifier output is connected to the record and playback system and to the spectrum analyzer for monitoring.

With this setup, non negligible third harmonic is generated by CW1 at 1575.75 MHz (harmonic power = -52 dBm). CW2 produces a spectral line at 1579.33 MHz that is 3.58 MHz apart from the CW1's third harmonic. If the CW2 power is gradually increased (from -5 dBm to 5 dBm), the new spectral components at 1582.58 MHz and at 1586.16 MHz appear on the spectrum.

This is due to respectively the second and the third harmonic of the fundamental CW2. Let us estimate the interference signal power at the GPS antenna input. Based on the Friis equation, the received by GPS antenna power can be expressed as following [12]:

$$P_R = P_T + G_T + G_R - L + 20\log_{10}\left(\frac{\lambda}{4\pi d}\right) \text{ [dBW] (0.8)}$$

where,

P_R Received power

P_T Transmitted power

G_R Receiver's antenna gain

G_T Transmitter's antenna gain

L System losses

λ Interference fundamental frequency

d Distance between the transmitter and receiver antenna

For simplicity, let us suppose an isotropic antenna for the transmitter/receiver side ($G_T = G_R = 0$ dB). All losses, including cable losses, impedance mismatch, antenna effectiveness, etc. are around 5dB. Transmitter power $P_T = 15$ dBm. If the distance d between the antennas is around 10 cm, the estimated received power P_R is:

$$P_R = 15 dBm - 5 dB + 20 \cdot \log_{10} \left(\frac{0.57}{4\pi \cdot 0.1} \right) \cong 3 dBm \ (0.9)$$

Assuming 50 dB of rejection by built-in RF pass-band filter, one should get around -47 dBm of power at the antenna LNA input. This is still more than 80 dB higher than expected at the LNA input (-130 dBm of power is expected at GPS antenna input). The power of the generated harmonics depends on the amplifier design that is proprietary for each manufacturer. Commonly, 40 dB of attenuation can be expected for second and third harmonics, compared to the fundamental frequency component. With this in mind, -87 dBm of power is expected for the third harmonic at the active antenna output. Considering 45 dB of preamplifier gain and 8 dB of overall losses (cables, filters, splitters, etc.), the expected harmonic's power should be around -50 dBm.

6. MAIN TEST AND ANALYSIS

To validate the proposed approach, the interference was generated under a controlled environment. As the source of interference, the UHF TV channel 23 was generated using Averna's video toolkit [13]. The UHF and GPS antenna were placed inside the shielded box to avoid the RF emissions on the air. The setup used is presented in Figure 10. In this test, the 3rd harmonic at the source was intentionally suppressed using a band-pass filter. This filter was calibrated and more than 100dB of the 3rd harmonic suppression was measured. The GPS active antenna is connected to the pre-amplifier which is a part of the recording system. The generated interference is also connected to the second recording channel directly (bypassing the pre-amplifier). Both signals (GPS antenna output and interference) were recorded on two recording channels.
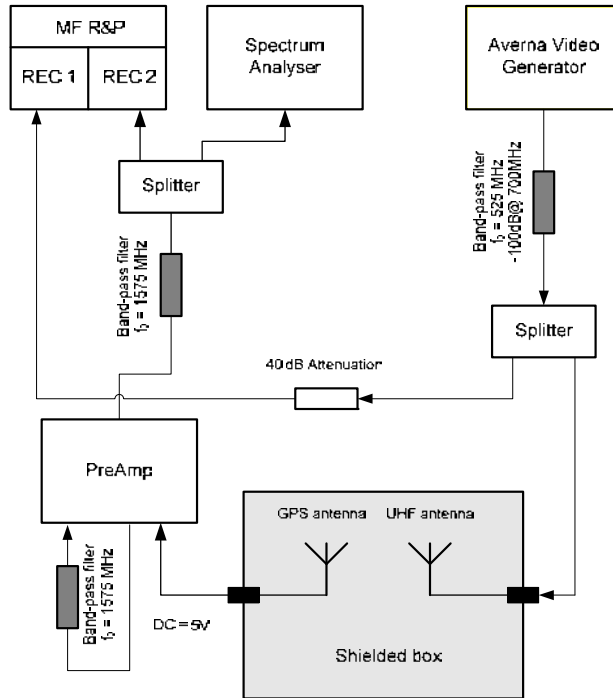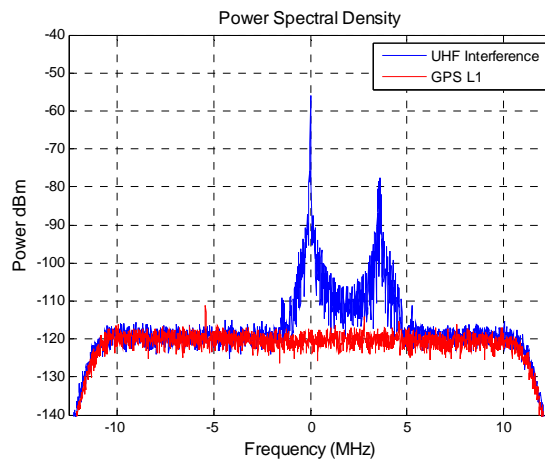
Figure 10 Test setup 2

Figure 11 Spectrum of the recorded Interference (525.14 MHz) and GPS signal (1575.42 MHz) transposed to baseband

Interference power of 0dBm at the generator output insures no visible traces of interference in the GPS L1 band (see Figure 11). For recording, the interference is intentionally attenuated.

Once recorded, the baseband signals are post-processed in Matlab for further analysis. The straight forward approach is to cross-correlate the recorded interference with the recorded GPS L1 signal. Also, the autocorrelation function is used to emphasize the interference's source signature.

Remember, the interference used for this validation test is a TV channel 23 that is NTSC video standard. One can expect to observe that the autocorrelation function of the interference should contain series of peaks spaced by ~1/60 s, ~1/15.7e3 s and ~1/3.58e6 s. In fact, these peaks are easily identified on the measured autocorrelation function.

The autocorrelation and cross-correlation function are presented in Figure 12. As expected, the measured autocorrelation's peaks (from Figure 12) are spaced by ~ 0.0637 ms which corresponds to ~15.7 kHz. Zooming on the correlation peak, the color subcarrier can be found (see Figure 13). Once again, the measurements show that the correlation peaks are spaced by ~0.28us which is equivalent to ~3.58 MHz of the color subcarrier. These particular characteristics of the autocorrelation function are used to simply identify the traces of the interference in the recorded GPS L1 signal.

Let us analyze more closely the cross-correlation function obtained from Figure 12. First of all, in the calculated cross-correlation function the correlation peaks are, as for interference autocorrelation function, spaced by exactly the same time interval (~ 0.0637 ms) for horizontal scanlines and the same time interval (~0.28us) for color subcarrier (Figure 15). This was somewhat unexpected as the cross-correlation was done with the fundamental frequency components (and not with the harmonics which is supposed to triple the frequencies at 3rd harmonic).

Once the interference was identified in the GPS L1 band, the power of this interference as well as the power of composite (GPS L1 + interference + noise) signal can be estimated using correlation function's properties [8] and the equations 1.4-1.7. The recorded GPS L1 signal power (GPS L1 + interference + noise) is estimated and the total power is -31dBm.

Based on the measured cross-correlation's peak value and equations 1.6-1.7, the power of the 3rd harmonic inside the GPS L1 band is around -65dBm. This is close to what was expected based on the first setup test (for the first setup, harmonic of -52dBm was observed with the 15dBm of the out off-band interference power. In the main test, the interference power was intentionally dropped to 0dBm that should lead to -67dBm for the 3rd harmonic's power).

This shows that the interference level inside the GPS L1 band is almost 34 dB lower than the composite (GPS + harmonic + noise) signal level. So, with 0 dBm of the interference power at the source (radiated antenna input), interference with -65 dBm is still present inside the GPS L1 band at the recorder input.
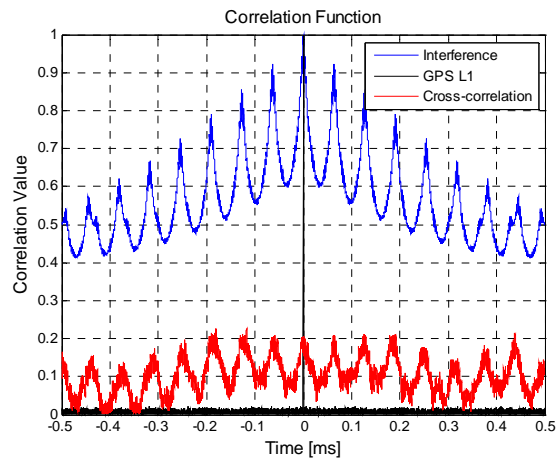
Figure 12 Correlation and cross-correlation functions for interference and GPS L1 signals
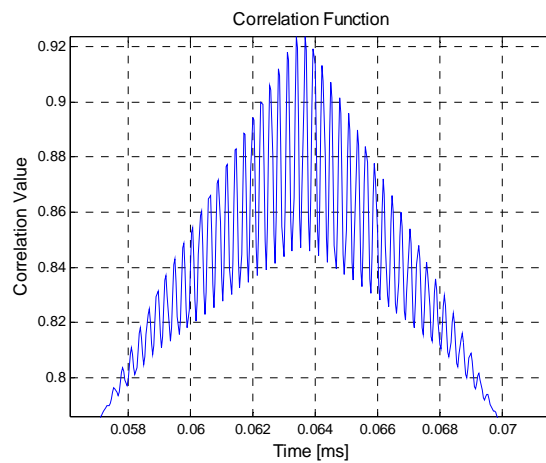

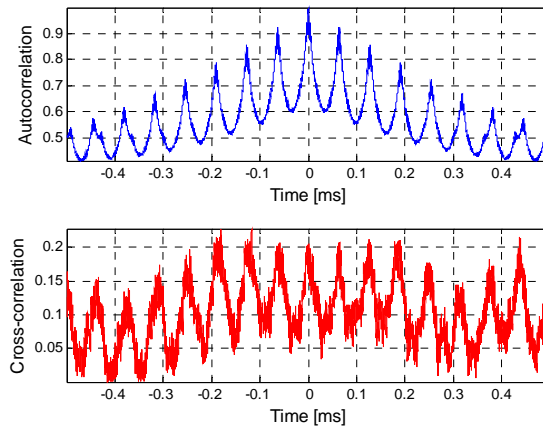*Figure 13 Autocorrelation function of color subcarrier*
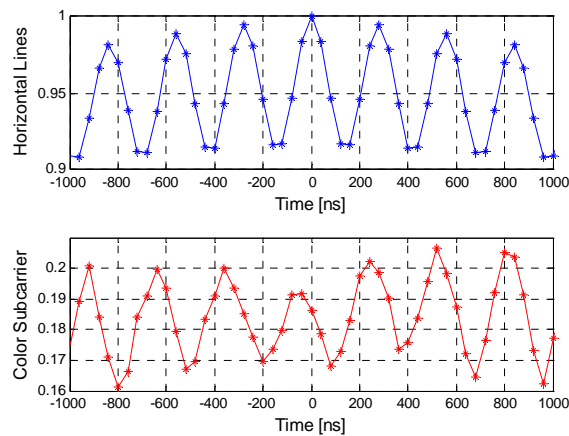
Figure 14 Correlation on horizontal scanlines

Figure 15 Correlation of color subcarrier

7. CONCLUSION

This paper presents a flexible and precise approach using inexpensive calculation solution to perform the detection and parameter's detection of UHF TV interferences using cross-correlation properties of harmful natural interferences. Future work would address the development of a database of potential interference signal structure for numerous kinds of interference to detect their presence and measured their real-time characteristic using the proposed low-cost approach.

The advantages of the demonstrated approach become obvious for real-time analysis using real signals, which is difficult and sometimes impossible to perform. In fact, real-time interference field tests analysis may be expensive and time consuming, especially when the interference analysis has to be done during flight tests or in hardly accessible areas.

Another advantage of the multiple-channel recording approach to interferences analysis is related to the design and validation of the anti-jamming algorithms. Repeatability of laboratory testing using real-world acquired signals is nowadays possible with high fidelity. New receiver architectures can be stressed in several recorded environment in the presence of live recorded GNSS signals combined with interferences (or multipath), ensuring the repeatability of the events. Once the GNSS and interference signals are recorded, the signal analysis can be done with maximum likelihood estimation approach or using software receiver with anti-jamming capabilities.

ACKNOWLEDGMENTS

REFERENCES

[1]   National Instruments, "NI T-Clock Technology for Timing and Synchronization of Modular Instruments," http://zone.ni.com/devzone/cda/tut/p/id/3675, Ed., 2008.

[2]   National Instruments, "NI PXIe-5663 6.6 GHz Vector Signal Analyzer," http://www.ni.com/pdf/products/us/cat_PXIe_5663.pdf, 2008.

[3]   National Instruments, "NI PXIe-5673 6.6 GHz Vector Signal Generator," http://www.ni.com/pdf/products/us/cat_PXIe_5673.pdf, 2008.

[4]   Averna Technologies Inc., "RF Signal Record & Playback System," http://www.averna.com/en/documents/brochures/averna_urt_rf_signal_record_playback_system_brochure.pdf, 2008.

[5]   Averna Technologies Inc., "Universal Receiver Tester," http://www.averna.com/en/products/universal_receiver_tester/index.php, 2008.

[6]   P. G. Ian Glover, *Digital Communications.* Europe: Prentice Hall, 1998.

[7]   J. G. Proakis, Manolakis, Dimitris G., *Digital Signal Processing: Principles, Algorithms, and Applications*, Third Edition ed. Upper Siddle River, New Jersey: Prentice Hall, 1996.

[8]   D. G. Manolakis, Ingle, Vinary K., Kogon, Stephen M., *Statistical and Adaptive Signal Processing.* Boston: Artech House, 2005.

[9]   B. W. Parkinson and J. J. Spilker, *The global positioning system : theory and applications*. Washington, DC: American Institute of Aeronautics and Astronautics, 1996.

[10]   Kaplan E. D. and C. Hegarty, *Understanding GPS : principles and applications*, 2nd ed. Boston: Artech House, 2006.

[11]   Landry Rene. Jr., "Analysis of Potential Interference Sources and Assessment of Present Solutions for GPS/GNSS Receivers," presented at 4th Saint-Petersburg on INS, Saint-Petersburg, 1997.

[12]   P. Misra and P. Enge, *Global positioning system : signals, measurements, and performance*. Lincoln, Mass.: Ganga-Jamuna Press, 2004.

[13]   Averna Technologies Inc., "NTSC/PAL RF Generator Toolkit," http://www.averna.com/en/documents/toolkits/video/urt_ntsc-pal_rf_generator_toolkit.pdf, Ed., 2009 ed, 2009.

Biography(s)

Iurie Ilie is a GPS specialist currently involved in the GNSS test equipment design and validation at Averna Technologies Inc. He received his Electrical Engineering Master's degree from *École de Technologie Supérieure* (Canada) in 2003. He has a strong experience in GPS signal processing and GPS receiver's testing. His current interests include software defined GNSS simulator's design and RF Record & Playback applications to GNSS.

Dominique Fortin is the Director of RF products at Averna where he leads the product line of RF generators. He received his bachelor degree in Electrical Engineering in 1985 at *Université de Sherbrooke* (Canada). He has worked in the field of Telecom and RF since he began his career.

René Jr. Landry received a B.Eng. degree in electronic at the École Polytechnique de Montréal (Montréal, Canada), in 1992, with a major in space technology. He also completed a M.Sc. in satellite communication engineering at the University of Surrey (Guildford, U.K.) in 1993, a Master in space electronics and a DEA (Diplôme d'Études Approfondies) in microwaves at the ENSAE/SupAero (Toulouse, France), in 1994. He obtained his Ph.D. degree at the University Paul-Sabatier and SupAéro (Toulouse, France), in 1997, in digital signal processing applied in navigation for anti-jamming technologies for the French civil aviation. Since 1999, Professor Landry has joined the ÉTS department of electrical engineering. His major interest concerns the development of new innovative mitigation techniques in non-ideal environment for GNSS receiver robustness design, including those of electronic inertial navigation systems based on low cost MEMs. He is actually working on several research projects in communication and sensor technologies, cognitive software-defined GNSS receiver, anti-jamming and robustness technologies, inertial navigation systems, augmentation systems, high precision and indoor navigation.

Marc-Antoine Fortin is currently pursuing his Ph.D. in the field of GNSS receivers' robustness field at the École de technologie supérieure (ÉTS) in Montréal, Canada. He previously received an Electrical Engineering Master's degree from the École Polytechnique de Montréal (Canada) in 2005 and a Bachelor's degree in the same field from the Université de Sherbrooke in 2003 (Canada). He is interested in new methods for universal GNSS acquisition and tracking to be used in severe environments with weak signal levels, multipath and interferences.

Contact us for a live demo

sales@averna.com OR 1-877-842-7577

Visit our website

www.averna.com/urt